Foraging depth depicts resource partitioning and contamination level in a pelagic shark assemblage: Insights from mercury stable isotopes

Lucien Besnard, Gaël Le Croizier, Felipe Galván-Magaña, David Point, Edouard Kraffe, James Ketchum, Raul Octavio Martinez Rincon, Gauthier Schaal

Version of Record: https://www.sciencedirect.com/science/article/pii/S0269749121006485
Manuscript_d31bb16673609e832084a3ca124afb21

Foraging depth depicts resource partitioning and contamination level in a pelagic shark assemblage: insights from mercury stable isotopes.

Lucien Besnard[1*], Gaël Le Croizier[1,2], Felipe Galván-Magaña[3], David Point[2], Edouard Kraffe[1], James Ketchum[4], Raul Octavio Martinez Rincon[5], Gauthier Schaal[1].

[1]Laboratoire des Sciences de l'Environnement Marin (LEMAR), UMR 6539 CNRS/UBO/IRD/IFREMER, BP 70, 29280 Plouzané, France

[2]UMR Géosciences Environnement Toulouse (GET), Observatoire Midi Pyrénées (OMP), 14 avenue Edouard Belin, 31400 Toulouse, France

[3]Instituto Politécnico Nacional, Centro Interdisciplinario de Ciencias Marinas, Av. IPN s/n, 23096 La Paz, B.C.S., México

[4]Pelagios-Kakunja, Cuauhtémoc 155, 23096 La Paz, B.C.S., México

[5]CONACyT-Centro de Investigaciónes Biológicas del Noroeste, S.C. (CIBNOR), Av. IPN 195, 23096 La Paz, B.C.S., México

*** Corresponding author at**: Laboratoire des Sciences de l'Environnement Marin (LEMAR), UMR 6539 CNRS/UBO/IRD/IFREMER, BP 70, 29280 Plouzané, France ; **E-mail address**: lbesnard.research@gmail.com (Lucien Besnard) ; **Phone number:** +33619251685 (France).

ABSTRACT

The decline of shark populations in the world ocean is affecting ecosystem structure and function in an unpredictable way and new ecological information is today needed to better understand shark roles in their habitats. In particular, the characterization of foraging patterns is crucial to understand and foresee the evolution of dynamics between sharks and their prey. Many shark species use the mesopelagic area as a major foraging ground but the degree to which different pelagic sharks rely on this habitat remains overlooked. In order to depict the vertical dimension of their trophic ecology, we used mercury stable isotopes in the muscle of three pelagic shark species (the blue shark *Prionace glauca*, the shortfin mako shark *Isurus oxyrinchus* and the smooth hammerhead shark *Sphyrna zygaena*) from the northeastern Pacific region. The Δ^{199}Hg values, ranging from 1.40 to 2.13 ‰ in sharks, suggested a diet mostly based on mesopelagic prey in oceanic habitats. We additionally used carbon and nitrogen stable isotopes (δ^{13}C, δ^{15}N) alone or in combination with Δ^{199}Hg values, to assess resource partitioning between the three shark species. Combining Δ^{199}Hg resulted in a decrease in trophic overlap estimates compared to δ^{13}C/δ^{15}N alone, demonstrating that multi-isotope modeling is needed for accurate trophic description of the three species. Mainly, it reveals that they forage at different average depths and that resource partitioning is mostly expressed through the vertical dimension within pelagic shark assemblages. Concomitantly, muscle total mercury concentration (THg) differed between species and increased with feeding depth. Overall, this study highlights the key role of the mesopelagic zone for shark species foraging among important depth gradients and reports new ecological information on trophic competition using mercury isotopes. It also suggests that foraging depth may play a pivotal role in the differences between muscle THg from co-occurring high trophic level shark species.

SUMMARY:

By analyzing the isotopic ratios of mercury, a major pollutant of marine ecosystems, this study characterized the foraging depth of three shark species. Feeding depth governed resource partitioning between species and explained mercury concentration in shark tissues.

1. INTRODUCTION

Sharks are facing worldwide a large variety of threats such as overfishing, pollution, ecosystem degradation and others (Dulvy et al., 2014; Hazen et al., 2013; Queiroz et al., 2019). In recent years, the decline of many shark populations in the global ocean has raised public concern due to the iconic nature of these top predators and their influence on marine ecosystems over various temporal and spatial scales (Ferretti et al., 2010; Heithaus et al., 2008). Since the consequences of their removal are difficult to assess and predict (Baum and Worm, 2009; Ferretti et al., 2010), ecological information on habitat use and foraging grounds are needed to better assess future changes in marine ecosystems (Shiffman et al., 2012).

Large sharks, such as most marine predators, influence their ecosystem mainly through trophic interactions, either by predation on mesopredators, i.e. top-down control (Baum and Worm, 2009; Ferretti et al., 2010), competition with sympatric (i.e. co-occurring) high trophic level predators (Matich et al., 2017), or more complex interactions (Heithaus et al., 2008; Jorgensen et al., 2019). Competition for a shared trophic resource can result in lower food availability, change in physiological condition, and ultimately, reduced fitness (Jorgensen et al., 2019). Therefore, evolutionary processes tend to favor resource partitioning in co-occurring top predators (Heithaus et al., 2013). Tracking studies have highlighted differences in habitat use between shark species suspected to compete for food (Meyer et al., 2010; Musyl et al., 2011), but this method appears limited to discriminate the diet of species sharing a same trophic ground. Isotopic trophic tracers, such as stable carbon and nitrogen isotopes, have been used to assess resource partitioning between sympatric predators (Heithaus et al., 2013). However, contrary to coastal ecosystems, pelagic trophic webs are most of the time based on phytoplankton production only resulting in homogeneous

isotopic signatures and in overlapping isotopic niches between predators (Kiszka et al., 2015; Klarian et al., 2018; Rosas-Luis et al., 2017). Rather than competition, overlapping regions of isotopic niches might therefore be due to some inherent approach limitations. For instance, stable isotopes have a poor ability to discriminate foraging depth for top-predators likely to feed in deep oceanic habitats (Choy et al., 2015; Kiszka et al., 2015) and only few studies have investigated the vertical dimension of resource partitioning in pelagic predator assemblages (Le Croizier et al., 2020b, 2020a).

The mesopelagic zone (200-1000 m below the ocean surface) contains one of the most important animal biomass on earth (Aksnes et al., 2017; Irigoien et al., 2014), principally gathered inside the "deep scattering layer" community (Costello and Breyer, 2017). It is mainly composed of fishes and invertebrates that are commonly targeted by marine megafauna (Aksnes et al., 2017; Davison et al., 2015; Hazen and Johnston, 2010). Among these predators, some pelagic shark species display typical deep diving patterns suggesting that they rely on this compartment, such as great white (Le Croizier et al., 2020a), blue (Braun et al., 2019) or scalloped hammerhead sharks (Jorgensen et al., 2009). Surprisingly, although the combined effect of climate change and fishing pressure is dramatically changing epipelagic fish biomass and dynamic (Pinsky et al., 2011; Tu et al., 2018), little attention has been paid to the mesopelagic zone which is also predicted to be affected by climate change (Proud et al., 2017). In this context, the importance of deeper mesopelagic prey for different oceanic shark species must be better assessed.

Mercury is a globally distributed atmospheric pollutant (Fitzgerald et al., 2007) having deleterious toxic effects on marine fauna (Eisler, 2006). Entering the ocean in its inorganic form, its bioavailability increases through methylation by microbial activity (Sunderland et al., 2009). The resulting methylmercury (MeHg) is incorporated and bioaccumulated, i.e. increase in concentration with age/length, naturally in marine organisms as well as biomagnified, i.e. increase in concentration with trophic position (Biton-Porsmoguer et al., 2018; Lavoie et al., 2013; Le Bourg et al., 2019). As long-lived predators at the top of food webs, sharks naturally exhibit high mercury concentrations

(Schartup et al., 2019), predominantly in the MeHg form (Carvalho et al., 2014; Kim et al., 2016; Storelli et al., 2003). Alongside these processes, mercury accumulation in marine predators appears to be also driven by other physiological (e.g. metabolism, ontogeny, detoxification mechanisms) (Bolea-Fernandez et al., 2019; Li et al., 2020), ecological (e.g. habitat, systems productivity, food web structure, foraging depth) (Ferriss and Essington, 2014; Lavoie et al., 2013; Le Croizier et al., 2019; Senn et al., 2010) and physical parameters (e.g. oxygen level, sea temperature) (Houssard et al., 2019; Le Bourg et al., 2019; Schartup et al., 2019). In the ocean, mercury is subject to mass-independent isotopic fractionation ("MIF", generally represented trough Δ^{199}Hg values) due to its photochemical transformation in the water column (Bergquist and Blum, 2007). Following light attenuation with depth, Δ^{199}Hg values decrease from the surface to aphotic waters (Blum et al., 2013). Δ^{199}Hg values are also not modified during trophic transfer between a prey and its predator (Kwon et al., 2016; Laffont et al., 2011), making this non-traditional isotope a powerful proxy to address trophic resources and feeding depth in marine predators (Le Croizier et al., 2020b; Madigan et al., 2018). Mercury isotopic composition is also affected by mass-dependent fractionation ("MDF"), studied through δ^{202}Hg values (Bergquist and Blum, 2007; Blum et al., 2013). δ^{202}Hg is modified during physico-chemical processes such as photoreduction (Bergquist and Blum, 2007) and volatilization (Zheng et al., 2007), but also during biological processes such as methylation (Janssen et al., 2016) and demethylation (Perrot et al., 2016). It is therefore a useful tool to study mercury metabolism in species capable of demethylating MeHg (Bolea-Fernandez et al., 2019; Li et al., 2020).

In this study, we used a combination of carbon, nitrogen and mercury stable isotope analyses to address resource partitioning in three sympatric pelagic shark species (blue, shortfin mako and smooth hammerhead sharks) off the west coast of the Baja California peninsula (Mexico) in the northeastern Pacific. Based on stomach contents and carbon and nitrogen stable isotopic analyses, these three species have previously been reported to display highly overlapping trophic niches (Klarian et al., 2018; Kone et al., 2014). However, because these sharks display different diving behavior patterns (Logan et al., 2020; Musyl et al., 2011; Santos and Coelho, 2018) leading to

different abilities to access potential prey in the mesopelagic layer, we tested the hypothesis that resource partitioning occurs along the vertical dimension of their habitat. From an ecological perspective, this would confirm the key importance of the mesopelagic compartment even for predators spending most of their time in the upper layers (Le Croizier et al., 2020b, 2020a). It would also highlight the limitations of studying only carbon and nitrogen isotopic composition in pelagic assemblages to assess the degree of trophic similarities and the importance of the addition of relevant biomarkers to better address resource partitioning. Finally, as vertical habitat has been suspected to influence mercury contamination in marine predators (Choy et al., 2009; Le Bourg et al., 2019), we evaluated if total mercury levels found in all three species could be related to foraging depth in sharks.

2. MATERIALS AND METHODS

2.1. Sampling strategy

From 2014 to 2016, samples were collected in the artisanal fishing camp of Punta Lobos (southern Baja California Sur, Mexico, northeast Pacific). Sharks were fished using long lines equipped with hooks. Sex and total length (TL) were recorded for each shark and approximately 1 g of muscle was extracted from the dorsal muscle between the first dorsal fin and snout. Immediately after collection, samples were transported to the laboratory on ice packs, preserved at -20 °C and freeze-dried prior to analysis. In total, 13 blue sharks (*Prionace glauca*), 10 shortfin mako sharks (*Isurus oxyrinchus*) and 13 smooth hammerhead sharks (*Sphyrna zygaena*) were sampled.

2.2. Carbon and nitrogen stable isotopes

Following the methodology proposed by Li et al., 2016b, two extractions were performed prior to isotopic ratio determination. To avoid $\delta^{13}C$ misinterpretation, lipids were extracted by placing each sample in 6 mL of a 2:1 chloroform:methanol Folch solution (Folch et al., 1957). Mechanical crushing using a Dounce homogenizer enhanced the extraction. The mixture was then

vortexed for 1 minute, left overnight at room temperature and centrifuged for another 10 minutes before tissue extraction. This process was repeated three times. For $\delta^{15}N$ determination, urea was also removed from the samples. Samples were immerged in 5 mL of distilled water, vortexed for 1 minute and left at room temperature for 24 hours. The aqueous phase was separated from the tissue after another 5 minutes centrifugation and this process was repeated three consecutive times. Samples were then re-dried and homogenized prior to analysis.

A sample of 0.50 mg of muscle powder was weighted into tin cups using a XPR10 microbalance (METTLER TOLEDO). Stable carbon and nitrogen isotope measurements were carried out using a continuous flow on a Thermo Scientific Flash EA 2000 elemental analyzer coupled to a Delta V Plus mass spectrometer (Pole Spectrométrie Océan, IUEM, Plouzané, France). Based on international standards (Vienna Pee Dee Belemnite for $\delta^{13}C$ and atmospheric nitrogen for $\delta^{15}N$), isotopic ratio (δ) are expressed in per mille (‰) following: $\delta X = ([R_{sample}/R_{standard}] - 1) \times 1000$ where X is ^{13}C or ^{15}N and R is the corresponding ratio $^{13}C/^{12}C$ or $^{15}N/^{14}N$. We repeatedly measured known international isotopic standards (i.e. IAEA-600 Caffeine, IAEA-CH-6 Sucrose, IAEA-N-1 and IAEA-N-2 Ammonium Sulphate) and an in-lab certified standard substance (i.e. Acetanilide) indicating analytical uncertainties of ± 0.23 ‰ for $\delta^{13}C$ and ± 0.16 ‰ for $\delta^{15}N$. C:N ratios for all samples were ranging from 3.07 to 3.36, validating good extractions as shown by Li et al., 2016b (i.e. mean C:N ratio after lipid and urea removal of 3.2 for blue and smooth hammerhead shark and 3.1 for shortfin mako shark).

2.3. Total mercury concentration

As total mercury concentration (THg) is known to be almost exclusively in the MeHg form in shark muscle, including for the species analyzed here, e.g. 95 to 98% in blue sharks (Carvalho et al., 2014; Kim et al., 2016; Storelli et al., 2003), THg was used as a proxy for MeHg. THg is expressed on a dry weight basis with an analytical detection limit of 0.005 $\mu g \cdot g^{-1}$ dw. A 20 mg aliquot section of dry muscle was analyzed using a DMA80 analyzer (Milestone, USA) after combustion, gold trapping and atomic absorption spectrophotometry detection. The analysis accuracy and reproducibility was

assessed from repeated measurements of two reference materials, a lobster hepatopancreas (TORT 3, NRCC, 0.292 ± 0.022 $\mu g \cdot g^{-1}$ dw) and a homogenate of tuna flesh (IAEA 436, INMM, 4.19 ± 0.36 $\mu g \cdot g^{-1}$ dw). Both reference materials were reproduced within the confidence limits (i.e. 0.286 ± 0.024 $\mu g \cdot g^{-1}$ dw for TORT 3, n = 10, and 4.20 ± 0.09 $\mu g \cdot g^{-1}$ dw for IAEA 436, n = 10).

2.4. Mercury isotopes

A segment of 20 mg of dry muscle was immersed into 3 mL of pure bi-distilled nitric acid (HNO_3) and left at room temperature overnight. Samples were then digested at 85°C for 6 hours in pyrolyzed glass vessels closed by Teflon caps on a hotplate. After the addition of 1 mL of hydrogen peroxide (H_2O_2), digestion continued for another 6 hours and 100 µL of BrCl were added to complete the extraction. Finally, the solution was diluted in an inverse aqua regia (3:1 HNO_3:HCl with 20 vol.% MilliQ water) to reach a total mercury concentration of 1 $ng \cdot mL^{-1}$.

Mercury isotopic compositions were measured at the Observatoire Midi-Pyrenées (Toulouse, France) using inductively coupled plasma mass spectrometry (MC−ICP−MS, Thermo Finnigan Neptune) with continuous-flow cold vapor (CV) generation using Sn(II) reduction (CETAC HGX-200), according to a previously published method (e.g. Le Croizier et al., 2020b). Mercury isotopic composition is expressed in δ notation, reported in per mil (‰) deviation from the NIST SRM 3133 standard and determined by sample-standard bracketing according to the following equation: $\delta^{XXX}Hg$ (‰) = $([(^{XXX}Hg/^{198}Hg)_{sample} / (^{XXX}Hg/^{198}Hg)_{standard}] - 1) \times 1000$ where XXX represents mercury isotope different masses. $\delta^{202}Hg$ represents Hg MDF, and Δ notation is used to express Hg MIF by the following equation: $\Delta^{XXX}Hg$ (‰) = $\delta^{XXX}Hg - (\delta^{202}Hg \times a)$ (Bergquist and Blum, 2007), where a = 0.252, 0.502, 0.752 and 1.493 for isotopes 199, 200, 201 and 204, respectively.

Blanks as well as certified materials (i.e. NRC TORT-3 and ERM-BCR-464) were analyzed with the same procedure. Total mercury concentration in the diluted digest mixtures was monitored by the ^{202}Hg signals provided by MC-ICP-MS. A recovery rate of 96 ± 7% (n = 37) for shark samples and 95 ± 6% (n = 7) for certified reference materials was obtained. Reproducibility of mercury isotope

174 measurements was assessed by analyzing UM-Almadén (n = 4), ETH-Fluka (n = 4) and the biological
175 tissue procedural standards NRC TORT-3 (n = 3) and ERM-BCR-464 (n = 4). Only one analysis was
176 performed per sample, but measured isotope signatures as well as analytical reproducibility of
177 standards agreed with previously published values (Table S1).

178 **2.5. Data analysis**

179 For comparison between shark species, data was first checked for normality using Shapiro–
180 Wilk test and for equality of variances using Bartlett's test. When both conditions were met, one-way
181 ANOVA were performed followed by a post-hoc Tukey's HSD test. Otherwise, we used its non-
182 parametric analogue, the Kruskal-Wallis test, followed by Dunn's post hoc test with Bonferroni's
183 adjustment in the presence of several groups. Between sexes comparisons (Student t test or its non-
184 parametric analogue Wilcoxon test) are described in Table S2.

185 We used 2D ($\delta^{13}C$ and $\delta^{15}N$) standard ellipse areas encompassing 95% of the data (SEA_B) calculated
186 using the SIBER package (Jackson et al., 2011) from R programming language (R Core Team, 2019). 3D
187 ($\delta^{13}C$, $\delta^{15}N$ and $\Delta^{199}Hg$) standard ellipsoid volumes encompassing 95% of the data (SEV_B) were
188 calculated using the SIBER-derived model described by Skinner et al., 2019, for three-dimensional
189 coordinate systems. To allow for comparison between the two model outputs, we expressed isotopic
190 overlap as a proportion of the non-overlapping area of the two 2D ellipses (SEA_B) or 3D ellipsoids
191 (SEV_B).

192 Pearson correlation test was used to describe the linear correlation between THg and $\Delta^{199}Hg$.
193 Generalized linear models (GLMs) were used to evaluate the influence of species, total length, C, N
194 and Hg isotope signatures on muscle mercury levels. GLMs were built with the LME4 package (Bates
195 et al., 2015) using THg as the response variable. Based on diagnostic plots of the residuals, a Gaussian
196 distribution and identity link function were used in the GLMs. Predictor variables were species, age,
197 $\delta^{13}C$, $\delta^{15}N$, $\Delta^{199}Hg$ and $\delta^{202}Hg$. Age was estimated for each individual using growth parameters
198 established for blue (Blanco-Parra et al., 2008), shortfin mako (Ribot-Carballal et al., 2005) and

smooth hammerhead sharks (Morán Villatoro et al., 2018) in the studied region. Models were built using backward stepwise selection which consists in building a model containing all predictor variables and removing gradually each predicator variable until no variable is left in the model (i.e. null model). Akaike's Information Criterion (AIC) was used to define the order of deletion as the model with the lowest AIC is retained for the next step. All models were ranked based on Akaike's Information Criterion adjusted for small sample sizes (AICc) and Akaike weights (w) using the R package WIQID (Meredith, 2020). Marginal R^2 were applied to assess each model predictive power using the R package R2GLMM (Jaeger, 2017).

3. RESULTS AND DISCUSSION

3.1. Carbon and nitrogen isotopic composition

A summary of the results is presented in Table 1. For all variables (TL, $\delta^{13}C$, $\delta^{15}N$, $\Delta^{199}Hg$, $\delta^{202}Hg$ and THg), no significant difference between sexes within species was detected (Table S2). In marine ecosystems, $\delta^{13}C$ is known to vary between habitats (e.g. coastal versus oceanic), according to primary producers supporting the food webs (e.g. benthic producers versus phytoplankton) (Fry and Sherr, 1984). Here, no significant difference in $\delta^{13}C$ was detected between the three species ($X^2_{35,2}$ = 6.1, p>0.05). These similarities in $\delta^{13}C$ profiles (Table 1) between the three species suggest that they forage on equivalent pelagic food webs derived from phytoplankton production, in accordance with reported data on shortfin mako and blue sharks in the study area (Hernández-Aguilar et al., 2016; Tamburin et al., 2019).

We found significant $\delta^{15}N$ differences among species ($F_{35,2}$ = 17.2, p<0.001). The smooth hammerhead shark presented significantly higher $\delta^{15}N$ than both the shortfin mako (Tukey's HSD test, p<0.05) and the blue shark (Tukey's HSD test, p<0.001). In contrast, the blue shark was ^{15}N depleted compared to the shortfin mako shark (Tukey's HSD test, p<0.05). In the case of mobile top-predator species evolving in the pelagic habitat, these differences in $\delta^{15}N$ can reflect either differences in relative trophic position (Cabana and Rasmussen, 1994) or foraging in different regions

with contrasted $\delta^{15}N$ baselines (Lorrain et al., 2015). In the northeastern Pacific region, no information is available on smooth hammerhead shark movement, while both blue and shortfin mako are known to perform limited horizontal movement without a clear seasonal pattern that could suggest foraging on broad different $\delta^{15}N$ ecosystem baselines (Musyl et al., 2011; Queiroz et al., 2019; Sepulveda et al., 2004). Therefore, their isotopic signatures likely represent an integrated signal of these shared habitat baselines. The significant differences observed in $\delta^{15}N$ signature between the three species might overall be due to differences in trophic levels, with blue sharks occupying the lowest trophic level and smooth hammerhead sharks the highest. In the study region, all three species are known to principally rely on different cephalopod species as observed in previous stomach content analyses. Shortfin mako sharks feed on *Dosidicus gigas* (Velasco Tarelo and Galván-Magaña, 2005), blue sharks on *Onychoteuthis banksii*, *Gonatus californiensis* and *D. gigas* and smooth hammerhead sharks on *D. gigas*, *Ancitrocheirus lesueurii* and *O. banksii* (Galván-Magaña et al., 2013). The apparent differences between the trophic levels of the three shark species could be the result of broad differences in cephalopods trophic levels. Indeed, the observed mean difference in $\delta^{15}N$ values between blue and smooth hammerhead sharks (2.15 ‰) matches the important variation in $\delta^{15}N$ signatures previously observed for cephalopod species sampled in the region (Madigan et al., 2012).

3.2. Inter-specific differences in foraging depth

Both $\Delta^{199}Hg$ and $\delta^{202}Hg$ signals vary vertically throughout the water column due to photochemical transformation of Hg following solar radiation decrease from surface to deep water layers (Bergquist and Blum, 2007; Blum et al., 2013). As they are transferred from prey to predator, they therefore can be used as trophic biomarkers to assess foraging depth. However, while $\Delta^{199}Hg$ is only affected through photochemical reactions and is conserved from prey to predator, $\delta^{202}Hg$ is also modified by physiological processes like methylation or demethylation of mercury (Bolea-Fernandez et al., 2019; Janssen et al., 2016; Li et al., 2020; Perrot et al., 2016) and undergoes inconstant trophic

discrimination factors from prey to predator (Kwon et al., 2016; Laffont et al., 2011), especially in shark species (Le Croizier et al., 2020b). Moreover, for blue, shortfin mako and smooth hammerhead sharks, metabolic MeHg detoxification pathways seems to occur. Indeed, the $\Delta^{199}Hg/\delta^{202}Hg$ slope is traditionally used to assess the influence of photodegradation *versus* microbial transformation on the isotopic signature of mercury before its incorporation into the food web (Blum et al., 2013; Madigan et al., 2018). Here, no significant linear regression could be obtained between $\Delta^{199}Hg$ and $\delta^{202}Hg$ for all shark species at the inter- or intraspecific level (Figure S1). This lack of correlation between $\Delta^{199}Hg$ and $\delta^{202}Hg$ is observed in species showing *in vivo* demethylation modifying the $\delta^{202}Hg$ values (Li et al., 2020) and suggests possible MeHg detoxification processes in the shark species studied here (Le Croizier et al., 2020b). Therefore, as $\delta^{202}Hg$ in all three shark species appeared to depend on both trophic and physiological features, this isotopic ratio was not taken into account to assess differences in species trophic ecology and subsequently to study the possible food competition between them.

In nearshore ecosystems, $\Delta^{199}Hg$ can vary seasonally and spatially due to coastal phenomena affecting water turbidity (Senn et al., 2010). In this study, the fact that all three shark species were pelagic species using oceanic habitats (as inferred by $\delta^{13}C$ values) confirms that reported $\Delta^{199}Hg$ may vary primarily over a vertical gradient depending on photochemical process affected by depth (Blum et al., 2013). Therefore, the range of individual $\Delta^{199}Hg$ values (1.40 to 2.13 ‰) observed in this study highlights the importance of mesopelagic prey in the diet of all three oceanic species. In the north Pacific oceanic region, similar $\Delta^{199}Hg$ signatures in fish muscles have been observed for species foraging in the twilight zone near Hawaii, i.e. 1.00 to 2.56 ‰ (Blum et al., 2013), and off the coast of California, i.e. 0.95 to 2.31 ‰ (Madigan et al., 2018), including for the great white shark, *Carcharodon carcharias*, i.e. 1.25 to 1.95 ‰ (Le Croizier et al., 2020a). This conclusion is supported by the consistent presence of mesopelagic species in stomach contents of blue (Hernández-Aguilar et al., 2016; Markaida and Sosa-Nishizaki, 2010), shortfin mako (Lopez et al., 2009; Preti et al., 2012) and smooth hammerhead sharks (Estupiñán-Montaño et al., 2019; Galván-Magaña et al., 2013) sampled off the west coast of Baja California and across the Pacific Ocean. As mercury has a similar

turnover rate as carbon and nitrogen in fish muscle, i.e. 1 year or more (Kwon et al., 2016), deep foraging appears as a constant strategy through time. The three shark species remain most of the time inside the boundaries of the surface mixed layer but exhibit differences in their diving behaviors in the study length range. Indeed, while blue sharks perform frequent deep dives (Campana et al., 2011; Queiroz et al., 2010), shortfin mako sharks seem to exploit deep water more sporadically undergoing less frequent dives in the mesopelagic zone (Abascal et al., 2011; Musyl et al., 2011). Finally, although no study reported depth habitat use in smooth hammerhead sharks in the Pacific region, data from the Atlantic Ocean demonstrated limited diving frequency associated with shallower dives than both shortfin mako and blue sharks (Logan et al., 2020; Santos and Coelho, 2018). Here, Δ^{199}Hg corroborates the deep diving behavior observed for blue and shortfin mako sharks and proves that they are associated with foraging in the mesopelagic layer. It also suggests that smooth hammerhead sharks might feed at depth and that populations from the northeastern Pacific region might differ from the Atlantic ones by using deeper water layers (Logan et al., 2020; Santos and Coelho, 2018).

We observed significant inter-specific differences in Δ^{199}Hg ratio ($X^2_{35,2}$ = 17.8, $p<0.001$) revealing differences in mean foraging depth. Blue sharks presented Δ^{199}Hg value significantly lower than shortfin mako sharks (Dunn's test, $p<0.001$) and smooth hammerhead sharks (Dunn's test, $p<0.01$). This could not be explained by different isotope fractionation between prey and predator, as Δ^{199}Hg values are conserved during trophic transfers (Kwon et al., 2016; Laffont et al., 2011). Thus, the significant gap in Δ^{199}Hg between species suggests systematic differences in foraging depths (Le Croizier et al., 2020b). The lower Δ^{199}Hg of the blue shark suggests constant foraging in deeper water than the two other species. This conclusion is supported by stomach content analyses, which revealed that this species was the only one with bathypelagic prey in its gut (Galván-Magaña et al., 2013). On the other hand, epipelagic prey were also commonly reported in the stomach of the three shark species (Galván-Magaña et al., 2013; Hernández-Aguilar et al., 2016; Wood et al., 2009). Δ^{199}Hg signatures observed in this study may thus be the result of the consumption of both epi- and

mesopelagic prey as reported for the Pacific bluefin tuna *Thunnus orientalis* (Madigan et al., 2018). Differences in the relative importance of prey from these two compartments could therefore result in the observed Δ^{199}Hg differences between shark species. Compared to deeper species, epipelagic prey may form dense aggregations with higher nutritive and energetic value (Madigan et al., 2018; Spitz et al., 2010). However, they are more scattered across time and space resulting in shark feeding opportunistically on them depending on the season, geographic position and maturity stage (Hernández-Aguilar et al., 2016; Maia et al., 2006; Rosas-Luis et al., 2017). This behavior is frequently observed in shortfin mako sharks, which favor a diet dominated by shallower teleost when seasonally and locally available (Harford, 2013; Maia et al., 2006). Compared to the shortfin mako, blue sharks display a more consistent diet targeting less nutritive but more reliable mesopelagic prey (Preti et al., 2012; Vollenweider et al., 2011). The mesopelagic food web indeed appears more stable through time and supports high prey biomasses in the northeast Pacific (Davison et al., 2015; Hazen and Johnston, 2010). Therefore, foraging on these deeper prey might represent a more reliable feeding strategy and involve less metabolic costs associated to foraging on more scattered epipelagic prey. Overall, the highest Δ^{199}Hg of blue sharks compared to shortfin mako sharks might be the result of different foraging strategies, with the blue shark occupying a deeper ecological niche and the shortfin mako shark favoring opportunistic foraging on epipelagic prey. Smooth hammerhead shark Δ^{199}Hg was not significantly different from the shortfin mako shark (Dunn's test, $p>0.05$), hence, suggesting feeding at shallower depths than blue sharks and/or at equivalent rates on deeper organisms than shortfin mako sharks.

3.3. Resource partitioning between co-occurring predators

The overlaps between the three species SEA_B (i.e. δ^{13}C and δ^{15}N, Figure 1) and SEV_B (i.e. δ^{13}C, δ^{15}N and Δ^{199}Hg, Figure 2) are presented in Table 2. The limited differences between δ^{13}C and δ^{15}N isotopic compositions resulted in significant isotopic overlaps between species except between blue and smooth hammerhead sharks (16.8%). The overlap decreased by adding Δ^{199}Hg for all pairs of

326 species. This decrease was the strongest for shortfin mako and blue sharks (from 42.0% to 23.0%). A
327 smaller overlap decrease was observed between shortfin mako and smooth hammerhead sharks,
328 which presented no significant difference in $\Delta^{199}Hg$, and between blue and smooth hammerhead
329 sharks, already well separated by $\delta^{15}N$ and to a less extent by $\delta^{13}C$ (i.e. 5.9% and 3.9% decrease
330 respectively). In the latter case, even if significant differences occurred in $\Delta^{199}Hg$, SEA_B and SEV_B
331 overlapping areas appeared equivalent suggesting that carbon and nitrogen isotopic ratios can be
332 sufficient to depict resource partitioning in the case of co-existing shark species feeding on different
333 habitats or prey (Curnick et al., 2019), although always overlooking the vertical dimension.

334 Resource partitioning within pelagic shark assemblages has been extensively studied using $\delta^{13}C$ and
335 $\delta^{15}N$, yielding frequent records of important overlapping areas (Kiszka et al., 2015; Li et al., 2016a)
336 suggesting similar foraging niches. In the eastern Pacific, similar overlaps were recorded between
337 shortfin mako and blue shark (Klarian et al., 2018; Rosas-Luis et al., 2017). From a methodological
338 perspective, these similarities could however be expected in the case of these pelagic species.
339 Indeed, by foraging in the same region and on similar phytoplankton derived food web, sympatric
340 pelagic sharks would exhibit similar $\delta^{13}C$ signatures (Bird et al., 2018), and possibly similar $\delta^{15}N$
341 depending on prey trophic position, even when feeding on different prey. The observed similarities in
342 carbon and nitrogen isotopic niches between blue and shortfin mako sharks (overlapping at 42.0%) in
343 this study may therefore be due to these processes, rather than to a clear similarity in dietary habits.
344 Moreover, important overlaps in isotopic signatures are not in accordance with previous stomach
345 content analysis of both species in the northeastern Pacific region (Preti et al., 2012; Rosas-Luis et al.,
346 2017). Hence, the differences in mean foraging depth between the two species increased resource
347 partitioning estimation between the blue shark and the shortfin mako shark (19.0% decrease in
348 overlapping area).

349 Our results therefore demonstrate that carbon and nitrogen isotopic signatures overestimate
350 overlapping areas by not reflecting the importance of foraging depth, which was estimated here by

Δ^{199}Hg. In the case of pelagic sharks migrating vertically, carbon and nitrogen stable isotopes analysis has shown some limitations in its capacity to address foraging depth issues. Indeed, even if vertical patterns in nitrogen isotopic baselines have been reported in zooplankton (Hannides et al., 2013), such patterns are rarely observed for top predators (Choy et al., 2015). However, the vertical foraging component has been suspected of critical importance in the ecology of marine predators. For example, computational models based on prey distribution systematically resulted in the emergence of vertical movements in tropical oceanic predatory fishes (Dagorn et al., 2000). Furthermore, in pelagic systems, differences in vertical movement patterns in sympatric top-predator species, including sharks, have already been demonstrated (Choy et al., 2015; Musyl et al., 2011). In our study, the systematic decreases in overlapping area for all pair of comparisons, after the incorporation of Δ^{199}Hg, demonstrates that differences in foraging depth better explain trophic niche partitioning between shark species.

3.4. Influence of foraging depth on mercury exposure

Muscle THg (Table 1) significantly differed among the three species ($X^2_{35,2}$ = 15.2, $p<0.001$). Blue sharks presented higher THg compared to shortfin mako (Dunn's test, $p<0.05$) and smooth hammerhead sharks (Dunn's test, $p<0.001$), as already observed in a previous study in the area (Maz-Courrau et al., 2012). The blue shark was the species presenting both higher THg and lower Δ^{199}Hg. Regardless of the species, THg was higher for individuals foraging on the deepest mesopelagic prey (i.e. exhibiting the lowest Δ^{199}Hg) as shown by the significant and negative correlation between the two variables (Figure 3). In the open Pacific Ocean, MeHg, the most bioavailable form of mercury, is mainly produced in the mesopelagic layer and especially in the Oxygen Minimum Zone (Blum et al., 2013; Fitzgerald et al., 2007). As MeHg is trophically incorporated in food webs, sharks feeding in the mesopelagic zone will be exposed to higher MeHg levels compared to shallow feeding sharks, as highlighted by our results. This is in agreement with previous observation on fish (Monteiro et al., 1996), sea birds (Thompson et al., 1998) and pelagic predators (Choy et al., 2009; Houssard et al.,

2019; Le Bourg et al., 2019; Madigan et al., 2018) that demonstrated higher mercury contamination in deeper foraging individuals or species.

In generalized linear models (GLMs), Δ^{199}Hg and species were the main factor explaining shark THg compared to other variables (Table S3), confirming that foraging depth was a key driver of shark mercury concentration in our dataset. Foraging depth has rarely been assessed in THg accumulation studies of marine predators except by qualitative approaches such as attributing a median depth of occurrence (Choy et al., 2009) or habitat preference (Le Bourg et al., 2019) to the studied species. It is interesting to note that this approach would not have been relevant for blue, shortfin mako and smooth hammerhead sharks that remain in the upper oceanic layers and occasionally undergo deep bounce dives to feed on mesopelagic prey (Abascal et al., 2011; Campana et al., 2009; Queiroz et al., 2010; Sepulveda et al., 2004). In our study, mercury isotopic composition offers new opportunities to implement quantitative approaches of foraging depth. As Δ^{199}Hg was the main driver of THg (along with species), we suggest that this factor should be investigated in future research regarding mercury accumulation patterns in elasmobranchs.

In shark species, the pattern observed for THg in muscular tissue has been generally linked to changes in trophic level, generally estimated through δ^{15}N values (Biton-Porsmoguer et al., 2018; Le Bourg et al., 2019). Here, δ^{15}N did not explain THg variation. Although the limited number of samples may not cover the entire spectrum of length and trophic levels for all shark species, influence of such small δ^{15}N spectrum on THg has been previously demonstrated (Le Croizier et al., 2019). This therefore implies that foraging depth could affect more significantly THg in pelagic shark species than their respective trophic levels, but further investigations at a specific level or with broader size and δ^{15}N range are needed to confirm this effect.

THg in marine organisms depends not only on trophic features (Ferriss and Essington, 2014; Le Bourg et al., 2019; Thompson et al., 1998) but also on species physiological characteristics such as longevity, metabolic, growth and feeding rates and/or possible detoxication processes (Bolea-Fernandez et al.,

2019; Houssard et al., 2019; Li et al., 2020; Senn et al., 2010). This can be seen in our results as the best-fitted model incorporated species as a key variable explaining THg (along with Δ^{199}Hg). However, all these parameters could not be tested in this study, except for longevity and demethylation mechanisms which are known to increase δ^{202}Hg values (Bolea-Fernandez et al., 2019; Senn et al., 2010). Here, δ^{202}Hg values varied significantly between species (Table 1; $F_{35,2}$ = 4.4, $p<0.05$), as previously observed for other co-occurring shark species (Le Croizier et al., 2020b). Still, δ^{202}Hg variations did not affect THg in GLMs (as it can also be seen in the relation between the two variables in Figure S2) showing no link between mercury contamination and the demethylation process previously highlighted by the absence of correlation between Δ^{199}Hg and δ^{202}Hg (Figure S1). Age was also not affecting THg while differences between species were also significant ($F_{35,2}$ = 8.6, $p<0.001$), with blue sharks encompassing the oldest individuals and shortfin mako sharks the youngest (Table S5). Overall, the fact that metabolic demethylation and individual age did not critically affect THg strengthens the hypothesis that ecological characteristics were mainly driving muscle mercury contamination in all shark species. As all physiological characteristics could not be analyzed in this study, future investigations on physiological intra-specific differences between blue, shortfin mako and smooth hammerhead sharks might help to identify the entire mechanisms behind their THg.

3.4. Insights into mercury cycle

In the northeastern Pacific region, atmospheric mercury deposition dominates mercury inputs to the water column as river influence appears negligible (Masbou et al., 2018; Zhang et al., 2014). This deposition at the atmosphere/ocean interface has two different origins: inorganic mercury (iHg) via precipitation and atmospheric gaseous mercury (Hg(0)) through dissolution (Gratz et al., 2010; Zhang et al., 2014). While the mechanisms causing mass-independent isotopic fractionation (MIF) of even-mass Hg isotopes are still poorly understood, processes such as photo-oxidation of Hg(0) to iHg in the atmosphere (e.g. tropopause) may be involved leading to isotopic fractionation (Chen et al., 2012). Therefore, iHg deposition by precipitation presents slightly different

Δ^{200}Hg signatures ranging from 0 to 0.3 ‰ than atmospheric Hg(0) dissolution characterized by Δ^{200}Hg between −0.11 and −0.01 ‰ (Enrico et al., 2016; Gratz et al., 2010). Once in the water column, Δ^{200}Hg values are conserved, making it a good tracer of atmospheric deposition pathways even when analyzed in top-predator species (Enrico et al., 2016; Le Croizier et al., 2020b). Here, Δ^{200}Hg values ranged from −0.07 to 0.14 ‰ with no significant differences between species ($F_{35,2}$ = 1.4, p>0.05; i.e. 0.05 ± 0.05 ‰ for blue and smooth hammerhead sharks and 0.02 ± 0.05 ‰ for shortfin mako sharks). These values are similar to those observed in bottomfish from Hawaii, i.e. −0.04 to 0.10 ‰ (Sackett et al., 2017), and to other coastal shark species sampled off La Réunion Island, i.e. 0.08 ± 0.04 ‰ in bull sharks, *Carcharhinus leucas*, and 0.06 ± 0.04 ‰ in tiger sharks, *Galeocerdo cuvier* (Le Croizier et al., 2020b). For the three shark species, Δ^{200}Hg values suggest a common origin in the mercury precursors of MeHg in shark tissues, probably from a combined source of both iHg and Hg(0) because of both positive and negative Δ^{200}Hg compositions (Le Croizier et al., 2020b).

Due to solar radiation, photodemethylation can transform dissolved MeHg into iHg and photoreduction can convert iHg into Hg(0) in the water column. Both of these reactions are characterized by a Δ^{199}Hg/Δ^{201}Hg ratio of respectively 1.36 and 1.00 (Bergquist and Blum, 2007). All shark species considered, Δ^{199}Hg/Δ^{201}Hg slope was 1.16 (Figure S3), not clearly indicating the prevalence of one reaction over another. Surprisingly this is not in accordance with previous studies reporting the dominance of MeHg demethylation in oceanic island marine ecosystems (Le Croizier et al., 2020b; Sackett et al., 2017). Indeed, the ratio observed here seems to represent a mixed signature of both phenomena. Interestingly, in Hawaii, deep-foraging species exhibit a flatter Δ^{199}Hg/Δ^{201}Hg slope (1.05 ratio) compared to shallower species (1.21 ratio) (Blum et al., 2013; Masbou et al., 2018). The intermediate slope in this study is therefore consistent with shark species foraging on mesopelagic prey exhibiting a flatter slope than epipelagic ones, reinforcing the conclusion that all three shark species foraged mainly at depth.

Conclusions

Based on $\delta^{13}C$, $\delta^{15}N$ and $\Delta^{199}Hg$, this study provided new information on the trophic ecology of blue, shortfin mako and smooth hammerhead sharks in the eastern Pacific region. Mesopelagic prey appeared as a major component in the diet of the three species. Our study demonstrated the importance of considering foraging depth when studying resource partitioning between co-occurring pelagic predators. In the northeastern Pacific, blue sharks appeared to forage deeper than mako and smooth hammerhead sharks and these foraging strategies seemed to reduce trophic competition between them. Since carbon and nitrogen isotopes did clearly underestimate resource partitioning, this study confirmed the usefulness of multi-isotopic approaches to help fine scaling resource partitioning in top-predators depending on the ecology of the studied species. Our results highlighted the underexploited potential of mercury stable isotopes for marine ecology studies. This new tool has the potential to elucidate possible ontogenetic variation in depth utilization for these species, as deep diving at early life stages is a rare pattern for blue and shortfin mako sharks (Nosal et al., 2019) and could be limited inside shallow coastal nursery areas for smooth hammerhead sharks (Francis, 2016; Santos and Coelho, 2018). Moreover, there are increasing evidences of vertical habitat partitioning between different predator species in other pelagic ecosystems (Madigan et al., 2020) and mercury stable isotopes could help to precise the mechanisms behind such vertical structuring. As foraging depth appeared a key factor influencing mercury exposure for the three species, it should be more extensively studied to understand mercury accumulation in top predators. In the context of climate change, Oxygen Minimum Zones are observed at shallower depth in tropical and subtropical regions, acting as a physical barrier and preventing sharks to forage deeper in the water column (Vedor et al., 2021), particularly in the tropical eastern Pacific (Trucco-Pignata et al., 2019). This habitat compression could therefore limit the possibility for co-occurring shark species to forage at significant different depths and could lead to new competition processes between pelagic predators that should be carefully monitored.

CRediT authorship contribution statement

Lucien Besnard: Conceptualization, Methodology, Formal analysis, Investigation, Writing - Original Draft, Writing - Review & Editing, Visualization. **Gaël Le Croizier:** Methodology, Validation, Investigation, Writing - Review & Editing, Supervision. **Felipe Galván-Magaña:** Investigation, Resources, Writing - Review & Editing, Funding acquisition. **David Point:** Resources, Writing - Review & Editing, Funding acquisition. **Edouard Kraffe:** Resources, Writing - Review & Editing, Funding acquisition. **James Ketchum:** Resources, Writing - Review & Editing, Funding acquisition. **Raul Octavio Martinez Rincon:** Formal analysis, Resources, Writing - Review & Editing, Funding acquisition. **Gauthier Schaal:** Resources, Writing - Review & Editing, Supervision, Funding acquisition.

Acknowledgements

Lucien Besnard doctoral grant was funded by the École Doctorale des Sciences de la Mer et du Littoral (EDSML) and by the Université de Bretagne Occidentale (UBO). The project is supported by ISblue project, interdisciplinary graduate school for the blue planet (ANR-17-EURE-0015) and co-funded by a grant from the French government under the program "Investissements d'Avenir". It is also backed by MIC ERASMUS+ and Ecos Annuies projects. Gaël Le Croizier was supported by a postdoctoral grant from the French National Research Institute for Sustainable Development (IRD). Mercury concentrations and stable isotopic analysis was financially supported by the French National Research Agency (project ANR-17-CE34-0010 MERTOX, PI David Point). Felipe Galván-Magaña thanks the Instituto Politecnico Nacional for fellowships (COFAA, EDI). The authors would like to thank the Centro Interdisciplinario de Ciencias Marinas and the Centro de Investigaciones Biológicas del Noroeste, S. C. for their contribution in shark tissue sampling and processing, especially Bertha Olivia Arredondo Vega, Olivia Arjona López and Rosa Linda Salgado Garcia.

REFERENCES

Abascal, F.J., Quintans, M., Ramos-Cartelle, A., Mejuto, J., 2011. Movements and environmental preferences of the shortfin mako, Isurus oxyrinchus, in the southeastern Pacific Ocean. Mar. Biol. 158, 1175–1184. https://doi.org/10.1007/s00227-011-1639-1

Aksnes, D.L., Røstad, A., Kaartvedt, S., Martinez, U., Duarte, C.M., Irigoien, X., 2017. Light penetration structures the deep acoustic scattering layers in the global ocean. Sci. Adv. 3, e1602468. https://doi.org/10.1126/sciadv.1602468

Bates, D., Mächler, M., Bolker, B., Walker, S., 2015. Fitting Linear Mixed-Effects Models Using lme4. J. Stat. Softw. 67, 1–48. https://doi.org/10.18637/jss.v067.i01

Baum, J.K., Worm, B., 2009. Cascading top-down effects of changing oceanic predator abundances. J. Anim. Ecol. 78, 699–714. https://doi.org/10.1111/j.1365-2656.2009.01531.x

Bergquist, B.A., Blum, J.D., 2007. Mass-Dependent and -Independent Fractionation of Hg Isotopes by Photoreduction in Aquatic Systems. Science 318, 417–420. https://doi.org/10.1126/science.1148050

Bird, C.S., Veríssimo, A., Magozzi, S., Abrantes, K.G., Aguilar, A., Al-Reasi, H., Barnett, A., Bethea, D.M., Biais, G., Borrell, A., Bouchoucha, M., Boyle, M., Brooks, E.J., Brunnschweiler, J., Bustamante, P., Carlisle, A., Catarino, D., Caut, S., Cherel, Y., Chouvelon, T., Churchill, D., Ciancio, J., Claes, J., Colaço, A., Courtney, D.L., Cresson, P., Daly, R., de Necker, L., Endo, T., Figueiredo, I., Frisch, A.J., Hansen, J.H., Heithaus, M., Hussey, N.E., Iitembu, J., Juanes, F., Kinney, M.J., Kiszka, J.J., Klarian, S.A., Kopp, D., Leaf, R., Li, Y., Lorrain, A., Madigan, D.J., Maljković, A., Malpica-Cruz, L., Matich, P., Meekan, M.G., Ménard, F., Menezes, G.M., Munroe, S.E.M., Newman, M.C., Papastamatiou, Y.P., Pethybridge, H., Plumlee, J.D., Polo-Silva, C., Quaeck-Davies, K., Raoult, V., Reum, J., Torres-Rojas, Y.E., Shiffman, D.S., Shipley, O.N., Speed, C.W., Staudinger, M.D., Teffer, A.K., Tilley, A., Valls, M., Vaudo, J.J., Wai, T.-C., Wells, R.J.D., Wyatt, A.S.J., Yool, A., Trueman, C.N., 2018. A global perspective on the trophic geography of sharks. Nat. Ecol. Evol. 2, 299–305. https://doi.org/10.1038/s41559-017-0432-z

Biton-Porsmoguer, S., Bănaru, D., Boudouresque, C.F., Dekeyser, I., Bouchoucha, M., Marco-Miralles, F., Lebreton, B., Guillou, G., Harmelin-Vivien, M., 2018. Mercury in blue shark (Prionace glauca) and shortfin mako (Isurus oxyrinchus) from north-eastern Atlantic: Implication for fishery management. Mar. Pollut. Bull. 127, 131–138. https://doi.org/10.1016/j.marpolbul.2017.12.006

Blanco-Parra, M. del P., Magaña, F.G., Farías, F.M., 2008. Age and growth of the blue shark, Prionace glauca Linnaeus, 1758, in the Northwest coast off Mexico. Rev. Biol. Mar. Oceanogr. 43, 513–520.

Blum, J.D., Popp, B.N., Drazen, J.C., Anela Choy, C., Johnson, M.W., 2013. Methylmercury production below the mixed layer in the North Pacific Ocean. Nat. Geosci. 6, 879–884. https://doi.org/10.1038/ngeo1918

Bolea-Fernandez, E., Rua-Ibarz, A., Krupp, E.M., Feldmann, J., Vanhaecke, F., 2019. High-precision isotopic analysis sheds new light on mercury metabolism in long-finned pilot whales (Globicephala melas). Sci. Rep. 9, 1–10. https://doi.org/10.1038/s41598-019-43825-z

Braun, C.D., Gaube, P., Sinclair-Taylor, T.H., Skomal, G.B., Thorrold, S.R., 2019. Mesoscale eddies release pelagic sharks from thermal constraints to foraging in the ocean twilight zone. Proc. Natl. Acad. Sci. 116, 17187–17192. https://doi.org/10.1073/pnas.1903067116

Cabana, G., Rasmussen, J.B., 1994. Modelling food chain structure and contaminant bioaccumulation using stable nitrogen isotopes. Nature 372, 255–257. https://doi.org/10.1038/372255a0

Campana, S.E., Dorey, A., Fowler, M., Joyce, W., Wang, Z., Wright, D., Yashayaev, I., 2011. Migration Pathways, Behavioural Thermoregulation and Overwintering Grounds of Blue Sharks in the Northwest Atlantic. PLOS ONE 6, e16854. https://doi.org/10.1371/journal.pone.0016854

Campana, S.E., Joyce, W., Manning, M.J., 2009. Bycatch and discard mortality in commercially caught blue sharks Prionace glauca assessed using archival satellite pop-up tags. Mar. Ecol. Prog. Ser. 387, 241–253. https://doi.org/10.3354/meps08109

Carvalho, G.G.A. de, Degaspari, I.A.M., Branco, V., Canário, J., Amorim, A.F. de, Kennedy, V.H., Ferreira, J.R., 2014. Assessment of Total and Organic Mercury Levels in Blue Sharks (Prionace

551 glauca) from the South and Southeastern Brazilian Coast. Biol. Trace Elem. Res. 159, 128–
552 134. https://doi.org/10.1007/s12011-014-9995-6
553 Chen, J., Hintelmann, H., Feng, X., Dimock, B., 2012. Unusual fractionation of both odd and even
554 mercury isotopes in precipitation from Peterborough, ON, Canada. Geochim. Cosmochim.
555 Acta 90, 33–46. https://doi.org/10.1016/j.gca.2012.05.005
556 Choy, C.A., Popp, B.N., Hannides, C.C.S., Drazen, J.C., 2015. Trophic structure and food resources of
557 epipelagic and mesopelagic fishes in the North Pacific Subtropical Gyre ecosystem inferred
558 from nitrogen isotopic compositions. Limnol. Oceanogr. 60, 1156–1171.
559 https://doi.org/10.1002/lno.10085
560 Choy, C.A., Popp, B.N., Kaneko, J.J., Drazen, J.C., 2009. The influence of depth on mercury levels in
561 pelagic fishes and their prey. Proc. Natl. Acad. Sci. 106, 13865–13869.
562 https://doi.org/10.1073/pnas.0900711106
563 Costello, M.J., Breyer, S., 2017. Ocean Depths: The Mesopelagic and Implications for Global Warming.
564 Curr. Biol. 27, R36–R38. https://doi.org/10.1016/j.cub.2016.11.042
565 Curnick, D.J., Carlisle, A.B., Gollock, M.J., Schallert, R.J., Hussey, N.E., 2019. Evidence for dynamic
566 resource partitioning between two sympatric reef shark species within the British Indian
567 Ocean Territory. J. Fish Biol. 94, 680–685. https://doi.org/10.1111/jfb.13938
568 Dagorn, L., Menczer, F., Bach, P., Olson, R.J., 2000. Co-evolution of movement behaviours by tropical
569 pelagic predatory fishes in response to prey environment: a simulation model. Ecol. Model.
570 134, 325–341. https://doi.org/10.1016/S0304-3800(00)00374-4
571 Davison, P., Lara-Lopez, A., Anthony Koslow, J., 2015. Mesopelagic fish biomass in the southern
572 California current ecosystem. Deep Sea Res. Part II Top. Stud. Oceanogr., CCE-LTER:
573 Responses of the California Current Ecosystem to Climate Forcing 112, 129–142.
574 https://doi.org/10.1016/j.dsr2.2014.10.007
575 Dulvy, N.K., Fowler, S.L., Musick, J.A., Cavanagh, R.D., Kyne, P.M., Harrison, L.R., Carlson, J.K.,
576 Davidson, L.N., Fordham, S.V., Francis, M.P., Pollock, C.M., Simpfendorfer, C.A., Burgess, G.H.,
577 Carpenter, K.E., Compagno, L.J., Ebert, D.A., Gibson, C., Heupel, M.R., Livingstone, S.R.,
578 Sanciangco, J.C., Stevens, J.D., Valenti, S., White, W.T., 2014. Extinction risk and conservation
579 of the world's sharks and rays. eLife 3, e00590. https://doi.org/10.7554/eLife.00590
580 Eisler, R., 2006. Mercury Hazards to Living Organisms. CRC Press.
581 https://doi.org/10.1201/9781420008838
582 Enrico, M., Roux, G.L., Marusczak, N., Heimbürger, L.-E., Claustres, A., Fu, X., Sun, R., Sonke, J.E.,
583 2016. Atmospheric Mercury Transfer to Peat Bogs Dominated by Gaseous Elemental Mercury
584 Dry Deposition. Environ. Sci. Technol. 50, 2405–2412.
585 https://doi.org/10.1021/acs.est.5b06058
586 Estupiñán-Montaño, C., Cedeño-Figueroa, L., Estupiñán-Ortiz, J.F., Galván-Magaña, F., Sandoval-
587 Londoño, A., Castañeda-Suarez, D., Polo-Silva, C.J., 2019. Feeding habits and trophic level of
588 the smooth hammerhead shark, Sphyrna zygaena (Carcharhiniformes: Sphyrnidae), off
589 Ecuador. J. Mar. Biol. Assoc. U. K. 99, 673–680. https://doi.org/10.1017/S0025315418000474
590 Ferretti, F., Worm, B., Britten, G.L., Heithaus, M.R., Lotze, H.K., 2010. Patterns and ecosystem
591 consequences of shark declines in the ocean. Ecol. Lett. 13, 1055–1071.
592 https://doi.org/10.1111/j.1461-0248.2010.01489.x
593 Ferriss, B.E., Essington, T.E., 2014. Does trophic structure dictate mercury concentrations in top
594 predators? A comparative analysis of pelagic food webs in the Pacific Ocean. Ecol. Model.
595 278, 18–28. https://doi.org/10.1016/j.ecolmodel.2014.01.029
596 Fitzgerald, W.F., Lamborg, C.H., Hammerschmidt, C.R., 2007. Marine Biogeochemical Cycling of
597 Mercury. Chem. Rev. 107, 641–662. https://doi.org/10.1021/cr050353m
598 Folch, J., Lees, M., Sloane Stanley, G.H., 1957. A simple method for the isolation and purification of
599 total lipides from animal tissues. J. Biol. Chem. 226, 497–509.
600 Francis, M.P., 2016. Distribution, habitat and movement of juvenile smooth hammerhead sharks
601 (Sphyrna zygaena) in northern New Zealand. N. Z. J. Mar. Freshw. Res. 50, 506–525.
602 https://doi.org/10.1080/00288330.2016.1171244

Fry, B., Sherr, E.B., 1984. δ13C Measurements as Indicators of Carbon Flow in Marine and Freshwater Ecosystems, in: Rundel, P.W., Ehleringer, J.R., Nagy, K.A. (Eds.), Stable Isotopes in Ecological Research, Ecological Studies. Springer, New York, NY, pp. 196–229. https://doi.org/10.1007/978-1-4612-3498-2_12

Galván-Magaña, F., Polo-Silva, C., Berenice Hernández-Aguilar, S., Sandoval-Londoño, A., Ruth Ochoa-Díaz, M., Aguilar-Castro, N., Castañeda-Suárez, D., Cabrera Chavez-Costa, A., Baigorrí-Santacruz, Á., Eden Torres-Rojas, Y., Andrés Abitia-Cárdenas, L., 2013. Shark predation on cephalopods in the Mexican and Ecuadorian Pacific Ocean. Deep Sea Res. Part II Top. Stud. Oceanogr., The Role of Squids in Pelagic Ecosystems 95, 52–62. https://doi.org/10.1016/j.dsr2.2013.04.002

Gratz, L.E., Keeler, G.J., Blum, J.D., Sherman, L.S., 2010. Isotopic Composition and Fractionation of Mercury in Great Lakes Precipitation and Ambient Air. Environ. Sci. Technol. 44, 7764–7770. https://doi.org/10.1021/es100383w

Hannides, C.C.S., Popp, B.N., Choy, C.A., Drazen, J.C., 2013. Midwater zooplankton and suspended particle dynamics in the North Pacific Subtropical Gyre: A stable isotope perspective. Limnol. Oceanogr. 58, 1931–1946. https://doi.org/10.4319/lo.2013.58.6.1931

Harford, W.J., 2013. Trophic Modeling of Shortfin Mako (Isurus Oxyrinchus) and Bluefish (Pomatomus Saltatrix) Interactions in the Western North Atlantic Ocean. Bull. Mar. Sci. 89, 161–188. https://doi.org/info:doi/10.5343/bms.2011.1150

Hazen, E.L., Johnston, D.W., 2010. Meridional patterns in the deep scattering layers and top predator distribution in the central equatorial Pacific. Fish. Oceanogr. 19, 427–433. https://doi.org/10.1111/j.1365-2419.2010.00561.x

Hazen, E.L., Jorgensen, S., Rykaczewski, R.R., Bograd, S.J., Foley, D.G., Jonsen, I.D., Shaffer, S.A., Dunne, J.P., Costa, D.P., Crowder, L.B., Block, B.A., 2013. Predicted habitat shifts of Pacific top predators in a changing climate. Nat. Clim. Change 3, 234–238. https://doi.org/10.1038/nclimate1686

Heithaus, M.R., Frid, A., Wirsing, A.J., Worm, B., 2008. Predicting ecological consequences of marine top predator declines. Trends Ecol. Evol. 23, 202–210. https://doi.org/10.1016/j.tree.2008.01.003

Heithaus, M.R., Vaudo, J.J., Kreicker, S., Layman, C.A., Krützen, M., Burkholder, D.A., Gastrich, K., Bessey, C., Sarabia, R., Cameron, K., Wirsing, A., Thomson, J.A., Dunphy-Daly, M.M., 2013. Apparent resource partitioning and trophic structure of large-bodied marine predators in a relatively pristine seagrass ecosystem. Mar. Ecol. Prog. Ser. 481, 225–237. https://doi.org/10.3354/meps10235

Hernández-Aguilar, S.B., Escobar-Sánchez, O., Galván-Magaña, F., Abitia-Cárdenas, L.A., 2016. Trophic ecology of the blue shark (Prionace glauca) based on stable isotopes (δ13C and δ15N) and stomach content. J. Mar. Biol. Assoc. U. K. 96, 1403–1410. https://doi.org/10.1017/S0025315415001393

Houssard, P., Point, D., Tremblay-Boyer, L., Allain, V., Pethybridge, H., Masbou, J., Ferriss, B.E., Baya, P.A., Lagane, C., Menkes, C.E., Letourneur, Y., Lorrain, A., 2019. A Model of Mercury Distribution in Tuna from the Western and Central Pacific Ocean: Influence of Physiology, Ecology and Environmental Factors. Environ. Sci. Technol. 53, 1422–1431. https://doi.org/10.1021/acs.est.8b06058

Irigoien, X., Klevjer, T.A., Røstad, A., Martinez, U., Boyra, G., Acuña, J.L., Bode, A., Echevarria, F., Gonzalez-Gordillo, J.I., Hernandez-Leon, S., Agusti, S., Aksnes, D.L., Duarte, C.M., Kaartvedt, S., 2014. Large mesopelagic fishes biomass and trophic efficiency in the open ocean. Nat. Commun. 5, 1–10. https://doi.org/10.1038/ncomms4271

Jackson, A.L., Inger, R., Parnell, A.C., Bearhop, S., 2011. Comparing isotopic niche widths among and within communities: SIBER – Stable Isotope Bayesian Ellipses in R. J. Anim. Ecol. 80, 595–602. https://doi.org/10.1111/j.1365-2656.2011.01806.x

Jaeger, B., 2017. r2glmm: Computes R Squared for Mixed (Multilevel) Models.

654 Janssen, S.E., Schaefer, J.K., Barkay, T., Reinfelder, J.R., 2016. Fractionation of Mercury Stable
655 Isotopes during Microbial Methylmercury Production by Iron- and Sulfate-Reducing Bacteria.
656 Environ. Sci. Technol. 50, 8077–8083. https://doi.org/10.1021/acs.est.6b00854
657 Jorgensen, S.J., Anderson, S., Ferretti, F., Tietz, J.R., Chapple, T., Kanive, P., Bradley, R.W., Moxley,
658 J.H., Block, B.A., 2019. Killer whales redistribute white shark foraging pressure on seals. Sci.
659 Rep. 9, 6153. https://doi.org/10.1038/s41598-019-39356-2
660 Jorgensen, S.J., Klimley, A.P., Muhlia-Melo, A.F., 2009. Scalloped hammerhead shark Sphyrna lewini,
661 utilizes deep-water, hypoxic zone in the Gulf of California. J. Fish Biol. 74, 1682–1687.
662 https://doi.org/10.1111/j.1095-8649.2009.02230.x
663 Kim, S.-J., Lee, H.-K., Badejo, A.C., Lee, W.-C., Moon, H.-B., 2016. Species-specific accumulation of
664 methyl and total mercury in sharks from offshore and coastal waters of Korea. Mar. Pollut.
665 Bull. 102, 210–215. https://doi.org/10.1016/j.marpolbul.2015.11.038
666 Kiszka, J.J., Aubail, A., Hussey, N.E., Heithaus, M.R., Caurant, F., Bustamante, P., 2015. Plasticity of
667 trophic interactions among sharks from the oceanic south-western Indian Ocean revealed by
668 stable isotope and mercury analyses. Deep Sea Res. Part Oceanogr. Res. Pap. 96, 49–58.
669 https://doi.org/10.1016/j.dsr.2014.11.006
670 Klarian, S.A., Canales-Cerro, C., Barría, P., Zárate, P., Concha, F., Hernández, S., Heidemeyer, M.,
671 Sallaberry-Pincheira, P., Meléndez, R., 2018. New insights on the trophic ecology of blue
672 (Prionace glauca) and shortfin mako sharks (Isurus oxyrinchus) from the oceanic eastern
673 South Pacific. Mar. Biol. Res. 14, 173–182. https://doi.org/10.1080/17451000.2017.1396344
674 Kone, A., Agnissan, J.-P.A., Kouassi, S.K., N'da, K., 2014. Diet of two sharks: Sphyrna zygeana
675 (Linnaeus, 1758) and Isurus oxyrinchus (Rafinesque, 1809) of the Ivorian coast. Int. J. Innov.
676 Appl. Stud. 8, 1173–1186.
677 Kwon, S.Y., Blum, J.D., Madigan, D.J., Block, B.A., Popp, B.N., 2016. Quantifying mercury isotope
678 dynamics in captive Pacific bluefin tuna (*Thunnus orientalis*). Elem Sci Anth 4, 000088.
679 https://doi.org/10.12952/journal.elementa.000088
680 Laffont, L., Sonke, J.E., Maurice, L., Monrroy, S.L., Chincheros, J., Amouroux, D., Behra, P., 2011. Hg
681 Speciation and Stable Isotope Signatures in Human Hair As a Tracer for Dietary and
682 Occupational Exposure to Mercury. Environ. Sci. Technol. 45, 9910–9916.
683 https://doi.org/10.1021/es202353m
684 Lavoie, R.A., Jardine, T.D., Chumchal, M.M., Kidd, K.A., Campbell, L.M., 2013. Biomagnification of
685 Mercury in Aquatic Food Webs: A Worldwide Meta-Analysis. Environ. Sci. Technol. 47,
686 13385–13394. https://doi.org/10.1021/es403103t
687 Le Bourg, B., Kiszka, J.J., Bustamante, P., Heithaus, M.R., Jaquemet, S., Humber, F., 2019. Effect of
688 body length, trophic position and habitat use on mercury concentrations of sharks from
689 contrasted ecosystems in the southwestern Indian Ocean. Environ. Res. 169, 387–395.
690 https://doi.org/10.1016/j.envres.2018.11.024
691 Le Croizier, G., Lorrain, A., Sonke, J.E., Hoyos-Padilla, E.M., Galván-Magaña, F., Santana-Morales, O.,
692 Aquino-Baleytó, M., Becerril-García, E.E., Muntaner-López, G., Ketchum, J., Block, B., Carlisle,
693 A., Jorgensen, S.J., Besnard, L., Jung, A., Schaal, G., Point, D., 2020a. The Twilight Zone as a
694 Major Foraging Habitat and Mercury Source for the Great White Shark. Environ. Sci. Technol.
695 https://doi.org/10.1021/acs.est.0c05621
696 Le Croizier, G., Lorrain, A., Sonke, J.E., Jaquemet, S., Schaal, G., Renedo, M., Besnard, L., Cherel, Y.,
697 Point, D., 2020b. Mercury isotopes as tracers of ecology and metabolism in two sympatric
698 shark species. Environ. Pollut. 265, 114931. https://doi.org/10.1016/j.envpol.2020.114931
699 Le Croizier, G., Schaal, G., Point, D., Le Loc'h, F., Machu, E., Fall, M., Munaron, J.-M., Boyé, A., Walter,
700 P., Laë, R., Tito De Morais, L., 2019. Stable isotope analyses revealed the influence of foraging
701 habitat on mercury accumulation in tropical coastal marine fish. Sci. Total Environ. 650,
702 2129–2140. https://doi.org/10.1016/j.scitotenv.2018.09.330
703 Li, M., Juang, C.A., Ewald, J.D., Yin, R., Mikkelsen, B., Krabbenhoft, D.P., Balcom, P.H., Dassuncao, C.,
704 Sunderland, E.M., 2020. Selenium and stable mercury isotopes provide new insights into

mercury toxicokinetics in pilot whales. Sci. Total Environ. 710, 136325. https://doi.org/10.1016/j.scitotenv.2019.136325
Li, Y., Zhang, Y., Dai, X., 2016a. Trophic interactions among pelagic sharks and large predatory teleosts in the northeast central Pacific. J. Exp. Mar. Biol. Ecol. 483, 97–103. https://doi.org/10.1016/j.jembe.2016.04.013
Li, Y., Zhang, Y., Hussey, N.E., Dai, X., 2016b. Urea and lipid extraction treatment effects on δ15N and δ13C values in pelagic sharks. Rapid Commun. Mass Spectrom. 30, 1–8. https://doi.org/10.1002/rcm.7396
Logan, R.K., Vaudo, J.J., Sousa, L.L., Sampson, M., Wetherbee, B.M., Shivji, M.S., 2020. Seasonal Movements and Habitat Use of Juvenile Smooth Hammerhead Sharks in the Western North Atlantic Ocean and Significance for Management. Front. Mar. Sci. 7. https://doi.org/10.3389/fmars.2020.566364
Lopez, S., Meléndez, R., Barría, P., 2009. Alimentación del tiburón marrajo Isurus oxyrinchus Rafinesque, 1810 (Lamniformes: Lamnidae) en el Pacífico suroriental. Rev. Biol. Mar. Oceanogr. 44, 439–451. https://doi.org/10.4067/S0718-19572009000200017
Lorrain, A., Graham, B.S., Popp, B.N., Allain, V., Olson, R.J., Hunt, B.P.V., Potier, M., Fry, B., Galván-Magaña, F., Menkes, C.E.R., Kaehler, S., Ménard, F., 2015. Nitrogen isotopic baselines and implications for estimating foraging habitat and trophic position of yellowfin tuna in the Indian and Pacific Oceans. Deep Sea Res. Part II Top. Stud. Oceanogr., Impacts of climate on marine top predators 113, 188–198. https://doi.org/10.1016/j.dsr2.2014.02.003
Madigan, D.J., Carlisle, A.B., Dewar, H., Snodgrass, O.E., Litvin, S.Y., Micheli, F., Block, B.A., 2012. Stable Isotope Analysis Challenges Wasp-Waist Food Web Assumptions in an Upwelling Pelagic Ecosystem. Sci. Rep. 2, 654. https://doi.org/10.1038/srep00654
Madigan, D.J., Li, M., Yin, R., Baumann, H., Snodgrass, O.E., Dewar, H., Krabbenhoft, D.P., Baumann, Z., Fisher, N.S., Balcom, P., Sunderland, E.M., 2018. Mercury Stable Isotopes Reveal Influence of Foraging Depth on Mercury Concentrations and Growth in Pacific Bluefin Tuna. Environ. Sci. Technol. 52, 6256–6264. https://doi.org/10.1021/acs.est.7b06429
Madigan, D.J., Richardson, A.J., Carlisle, A.B., Weber, S.B., Brown, J., Hussey, N.E., 2020. Water column structure defines vertical habitat of twelve pelagic predators in the South Atlantic. ICES J. Mar. Sci. https://doi.org/10.1093/icesjms/fsaa222
Maia, A., Queiroz, N., Correia, J.P., Cabral, H., 2006. Food habits of the shortfin mako, Isurus oxyrinchus , off the southwest coast of Portugal. Environ. Biol. Fishes 77, 157–167. https://doi.org/10.1007/s10641-006-9067-7
Markaida, U., Sosa-Nishizaki, O., 2010. Food and feeding habits of the blue shark Prionace glauca caught off Ensenada, Baja California, Mexico, with a review on its feeding. J. Mar. Biol. Assoc. U. K. 90, 977–994. https://doi.org/10.1017/S0025315409991597
Masbou, J., Sonke, J.E., Amouroux, D., Guillou, G., Becker, P.R., Point, D., 2018. Hg-Stable Isotope Variations in Marine Top Predators of the Western Arctic Ocean. ACS Earth Space Chem. 2, 479–490. https://doi.org/10.1021/acsearthspacechem.8b00017
Matich, P., Ault, J.S., Boucek, R.E., Bryan, D.R., Gastrich, K.R., Harvey, C.L., Heithaus, M.R., Kiszka, J.J., Paz, V., Rehage, J.S., Rosenblatt, A.E., 2017. Ecological niche partitioning within a large predator guild in a nutrient-limited estuary. Limnol. Oceanogr. 62, 934–953. https://doi.org/10.1002/lno.10477
Maz-Courrau, A., López-Vera, C., Galván-Magaña, F., Escobar-Sánchez, O., Rosíles-Martínez, R., Sanjuán-Muñoz, A., 2012. Bioaccumulation and Biomagnification of Total Mercury in Four Exploited Shark Species in the Baja California Peninsula, Mexico. Bull. Environ. Contam. Toxicol. 88, 129–134. https://doi.org/10.1007/s00128-011-0499-1
Meredith, M., 2020. wiqid: Quick and Dirty Estimates for Wildlife Populations.
Meyer, C.G., Papastamatiou, Y.P., Holland, K.N., 2010. A multiple instrument approach to quantifying the movement patterns and habitat use of tiger (Galeocerdo cuvier) and Galapagos sharks (Carcharhinus galapagensis) at French Frigate Shoals, Hawaii. Mar. Biol. 157, 1857–1868. https://doi.org/10.1007/s00227-010-1457-x

Monteiro, L., Costa, V., Furness, R., Santos, R., 1996. Mercury concentrations in prey fish indicate enhanced bioaccumulation in mesopelagic environments. Mar. Ecol. Prog. Ser. 141, 21–25. https://doi.org/10.3354/meps141021

Morán Villatoro, J.M., Galvan-Magaña, F., Hernández Herrera, A., 2018. Edad y crecimiento del tiburon martillo Sphyrna zygaena (LINNAEUS, 1758) en la costa occidental de baja california sur. (Thesis). Instituto Politécnico Nacional. Centro Interdisciplinario de Ciencias Marinas.

Musyl, M.K., Brill, R.W., Curran, D.S., Fragoso, N.M., McNaughton, L.M., Nielsen, A., Kikkawa, B.S., Moyes, C.D., 2011. Postrelease survival, vertical and horizontal movements, and thermal habitats of five species of pelagic sharks in the central Pacific Ocean. Fish. Bull. 109, 341–369.

Nosal, A.P., Cartamil, D.P., Wegner, N.C., Lam, C.H., Hastings, P.A., 2019. Movement ecology of young-of-the-year blue sharks Prionace glauca and shortfin makos Isurus oxyrinchus within a putative binational nursery area. Mar. Ecol. Prog. Ser. 623, 99–115. https://doi.org/10.3354/meps13021

Perrot, V., Masbou, J., Pastukhov, M.V., Epov, V.N., Point, D., Bérail, S., Becker, P.R., Sonke, J.E., Amouroux, D., 2016. Natural Hg isotopic composition of different Hg compounds in mammal tissues as a proxy for in vivo breakdown of toxic methylmercury. Metallomics 8, 170–178. https://doi.org/10.1039/C5MT00286A

Pinsky, M.L., Jensen, O.P., Ricard, D., Palumbi, S.R., 2011. Unexpected patterns of fisheries collapse in the world's oceans. Proc. Natl. Acad. Sci. 108, 8317–8322. https://doi.org/10.1073/pnas.1015313108

Preti, A., Soykan, C.U., Dewar, H., Wells, R.J.D., Spear, N., Kohin, S., 2012. Comparative feeding ecology of shortfin mako, blue and thresher sharks in the California Current. Environ. Biol. Fishes 95, 127–146. https://doi.org/10.1007/s10641-012-9980-x

Proud, R., Cox, M.J., Brierley, A.S., 2017. Biogeography of the Global Ocean's Mesopelagic Zone. Curr. Biol. 27, 113–119. https://doi.org/10.1016/j.cub.2016.11.003

Queiroz, N., Humphries, N.E., Couto, A., Vedor, M., da Costa, I., Sequeira, A.M.M., Mucientes, G., Santos, A.M., Abascal, F.J., Abercrombie, D.L., Abrantes, K., Acuña-Marrero, D., Afonso, A.S., Afonso, P., Anders, D., Araujo, G., Arauz, R., Bach, P., Barnett, A., Bernal, D., Berumen, M.L., Bessudo Lion, S., Bezerra, N.P.A., Blaison, A.V., Block, B.A., Bond, M.E., Bonfil, R., Bradford, R.W., Braun, C.D., Brooks, E.J., Brooks, A., Brown, J., Bruce, B.D., Byrne, M.E., Campana, S.E., Carlisle, A.B., Chapman, D.D., Chapple, T.K., Chisholm, J., Clarke, C.R., Clua, E.G., Cochran, J.E.M., Crochelet, E.C., Dagorn, L., Daly, R., Cortés, D.D., Doyle, T.K., Drew, M., Duffy, C.A.J., Erikson, T., Espinoza, E., Ferreira, L.C., Ferretti, F., Filmalter, J.D., Fischer, G.C., Fitzpatrick, R., Fontes, J., Forget, F., Fowler, M., Francis, M.P., Gallagher, A.J., Gennari, E., Goldsworthy, S.D., Gollock, M.J., Green, J.R., Gustafson, J.A., Guttridge, T.L., Guzman, H.M., Hammerschlag, N., Harman, L., Hazin, F.H.V., Heard, M., Hearn, A.R., Holdsworth, J.C., Holmes, B.J., Howey, L.A., Hoyos, M., Hueter, R.E., Hussey, N.E., Huveneers, C., Irion, D.T., Jacoby, D.M.P., Jewell, O.J.D., Johnson, R., Jordan, L.K.B., Jorgensen, S.J., Joyce, W., Keating Daly, C.A., Ketchum, J.T., Klimley, A.P., Kock, A.A., Koen, P., Ladino, F., Lana, F.O., Lea, J.S.E., Llewellyn, F., Lyon, W.S., MacDonnell, A., Macena, B.C.L., Marshall, H., McAllister, J.D., McAuley, R., Meÿer, M.A., Morris, J.J., Nelson, E.R., Papastamatiou, Y.P., Patterson, T.A., Peñaherrera-Palma, C., Pepperell, J.G., Pierce, S.J., Poisson, F., Quintero, L.M., Richardson, A.J., Rogers, P.J., Rohner, C.A., Rowat, D.R.L., Samoilys, M., Semmens, J.M., Sheaves, M., Shillinger, G., Shivji, M., Singh, S., Skomal, G.B., Smale, M.J., Snyders, L.B., Soler, G., Soria, M., Stehfest, K.M., Stevens, J.D., Thorrold, S.R., Tolotti, M.T., Towner, A., Travassos, P., Tyminski, J.P., Vandeperre, F., Vaudo, J.J., Watanabe, Y.Y., Weber, S.B., Wetherbee, B.M., White, T.D., Williams, S., Zárate, P.M., Harcourt, R., Hays, G.C., Meekan, M.G., Thums, M., Irigoien, X., Eguiluz, V.M., Duarte, C.M., Sousa, L.L., Simpson, S.J., Southall, E.J., Sims, D.W., 2019. Global spatial risk assessment of sharks under the footprint of fisheries. Nature 572, 461–466. https://doi.org/10.1038/s41586-019-1444-4

807 Queiroz, N., Humphries, N.E., Noble, L.R., Santos, A.M., Sims, D.W., 2010. Short-term movements and
808 diving behaviour of satellite-tracked blue sharks Prionace glauca in the northeastern Atlantic
809 Ocean. Mar. Ecol. Prog. Ser. 406, 265–279. https://doi.org/10.3354/meps08500
810 R Core Team, 2019. R: A language and environment for statistical computing. R Foundation for
811 Statistical Computing, Vienna, Austria.
812 Ribot-Carballal, M.C., Galván-Magaña, F., Quiñónez-Velázquez, C., 2005. Age and growth of the
813 shortfin mako shark, Isurus oxyrinchus, from the western coast of Baja California Sur, Mexico.
814 Fish. Res. 76, 14–21. https://doi.org/10.1016/j.fishres.2005.05.004
815 Rosas-Luis, R., Navarro, J., Loor-Andrade, P., Forero, M.G., 2017. Feeding ecology and trophic
816 relationships of pelagic sharks and billfishes coexisting in the central eastern Pacific Ocean.
817 Mar. Ecol. Prog. Ser. 573, 191–201. https://doi.org/10.3354/meps12186
818 Sackett, D.K., Drazen, J.C., Popp, B.N., Choy, C.A., Blum, J.D., Johnson, M.W., 2017. Carbon, Nitrogen,
819 and Mercury Isotope Evidence for the Biogeochemical History of Mercury in Hawaiian
820 Marine Bottomfish. Environ. Sci. Technol. 51, 13976–13984.
821 https://doi.org/10.1021/acs.est.7b04893
822 Santos, C.C., Coelho, R., 2018. Migrations and habitat use of the smooth hammerhead shark (Sphyrna
823 zygaena) in the Atlantic Ocean. PLOS ONE 13, e0198664.
824 https://doi.org/10.1371/journal.pone.0198664
825 Schartup, A.T., Thackray, C.P., Qureshi, A., Dassuncao, C., Gillespie, K., Hanke, A., Sunderland, E.M.,
826 2019. Climate change and overfishing increase neurotoxicant in marine predators. Nature
827 572, 648–650. https://doi.org/10.1038/s41586-019-1468-9
828 Senn, D.B., Chesney, E.J., Blum, J.D., Bank, M.S., Maage, A., Shine, J.P., 2010. Stable Isotope (N, C, Hg)
829 Study of Methylmercury Sources and Trophic Transfer in the Northern Gulf of Mexico.
830 Environ. Sci. Technol. 44, 1630–1637. https://doi.org/10.1021/es902361j
831 Sepulveda, C.A., Kohin, S., Chan, C., Vetter, R., Graham, J.B., 2004. Movement patterns, depth
832 preferences, and stomach temperatures of free-swimming juvenile mako sharks, Isurus
833 oxyrinchus, in the Southern California Bight. Mar. Biol. 145, 191–199.
834 https://doi.org/10.1007/s00227-004-1356-0
835 Shiffman, D.S., Gallagher, A.J., Boyle, M.D., Hammerschlag-Peyer, C.M., Hammerschlag, N., 2012.
836 Stable isotope analysis as a tool for elasmobranch conservation research: a primer for non-
837 specialists. Mar. Freshw. Res. 63, 635–643. https://doi.org/10.1071/MF11235
838 Skinner, C., Mill, A.C., Newman, S.P., Newton, J., Cobain, M.R.D., Polunin, N.V.C., 2019. Novel tri-
839 isotope ellipsoid approach reveals dietary variation in sympatric predators. Ecol. Evol. 9,
840 13267–13277. https://doi.org/10.1002/ece3.5779
841 Spitz, J., Mourocq, E., Leauté, J.-P., Quéro, J.-C., Ridoux, V., 2010. Prey selection by the common
842 dolphin: Fulfilling high energy requirements with high quality food. J. Exp. Mar. Biol. Ecol.
843 390, 73–77. https://doi.org/10.1016/j.jembe.2010.05.010
844 Storelli, M.M., Ceci, E., Storelli, A., Marcotrigiano, G.O., 2003. Polychlorinated biphenyl, heavy metal
845 and methylmercury residues in hammerhead sharks: contaminant status and assessment.
846 Mar. Pollut. Bull. 46, 1035–1039. https://doi.org/10.1016/S0025-326X(03)00119-X
847 Sunderland, E.M., Krabbenhoft, D.P., Moreau, J.W., Strode, S.A., Landing, W.M., 2009. Mercury
848 sources, distribution, and bioavailability in the North Pacific Ocean: Insights from data and
849 models. Glob. Biogeochem. Cycles 23. https://doi.org/10.1029/2008GB003425
850 Tamburin, E., Kim, S.L., Elorriaga-Verplancken, F.R., Madigan, D.J., Hoyos-Padilla, M., Sánchez-
851 González, A., Hernández-Herrera, A., Castillo-Geniz, J.L., Godinez-Padilla, C.J., Galván-
852 Magaña, F., 2019. Isotopic niche and resource sharing among young sharks (Carcharodon
853 carcharias and Isurus oxyrinchus) in Baja California, Mexico. Mar. Ecol. Prog. Ser. 613, 107–
854 124. https://doi.org/10.3354/meps12884
855 Thompson, D.R., Furness, R.W., Monteiro, L.R., 1998. Seabirds as biomonitors of mercury inputs to
856 epipelagic and mesopelagic marine food chains. Sci. Total Environ. 213, 299–305.
857 https://doi.org/10.1016/S0048-9697(98)00103-X

858 Trucco-Pignata, P.N., Hernández-Ayón, J.M., Santamaria-del-Angel, E., Beier, E., Sánchez-Velasco, L.,
859 Godínez, V.M., Norzagaray, O., 2019. Ventilation of the Upper Oxygen Minimum Zone in the
860 Coastal Region Off Mexico: Implications of El Niño 2015–2016. Front. Mar. Sci. 6.
861 https://doi.org/10.3389/fmars.2019.00459
862 Tu, C.-Y., Chen, K.-T., Hsieh, C., 2018. Fishing and temperature effects on the size structure of
863 exploited fish stocks. Sci. Rep. 8, 1–10. https://doi.org/10.1038/s41598-018-25403-x
864 Vedor, M., Queiroz, N., Mucientes, G., Couto, A., Costa, I. da, Santos, A. dos, Vandeperre, F., Fontes,
865 J., Afonso, P., Rosa, R., Humphries, N.E., Sims, D.W., 2021. Climate-driven deoxygenation
866 elevates fishing vulnerability for the ocean's widest ranging shark. eLife 10, e62508.
867 https://doi.org/10.7554/eLife.62508
868 Velasco Tarelo, M.P., Galván-Magaña, F., 2005. Hábitos alimenticios e isótopos de 13C y 15N del
869 tiburón mako Isurus oxyrinchus (Rafinesque, 1810) en la costa occidental de Baja California
870 Sur (Thesis). Instituto Politécnico Nacional. Centro Interdisciplinario de Ciencias Marinas.
871 Vollenweider, J.J., Heintz, R.A., Schaufler, L., Bradshaw, R., 2011. Seasonal cycles in whole-body
872 proximate composition and energy content of forage fish vary with water depth. Mar. Biol.
873 158, 413–427. https://doi.org/10.1007/s00227-010-1569-3
874 Wood, A.D., Wetherbee, B.M., Juanes, F., Kohler, N.E., Wilga, C., 2009. Recalculated diet and daily
875 ration of the shortfin mako (Isurus oxyrinchus), with a focus on quantifying predation on
876 bluefish (Pomatomus saltatrix) in the northwest Atlantic Ocean. Fish. Bull. 107, 76–88.
877 Zhang, Y., Jaeglé, L., Thompson, L., 2014. Natural biogeochemical cycle of mercury in a global three-
878 dimensional ocean tracer model. Glob. Biogeochem. Cycles 28, 553–570.
879 https://doi.org/10.1002/2014GB004814
880 Zheng, W., Foucher, D., Hintelmann, H., 2007. Mercury isotope fractionation during volatilization of
881 Hg(0) from solution into the gas phase. J. Anal. At. Spectrom. 22, 1097–1104.
882 https://doi.org/10.1039/B705677J

FIGURES AND TABLES (*Colors should be used for any figures in the print*)

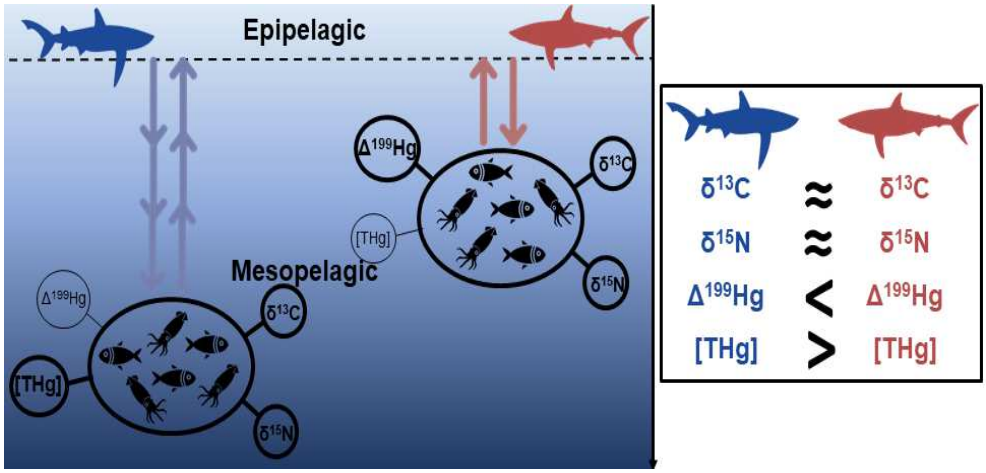

Graphical abstract

KEYWORDS

Trophic ecology; Top-predator; Mercury stable isotopes; Resource partitioning; Foraging depth; Mercury accumulation

HIGHLIGHTS

- $\delta^{13}C$, $\delta^{15}N$, $\Delta^{199}Hg$ and $\delta^{202}Hg$ were determined in three pelagic shark species.
- Hg isotopes suggested shark species foraged on mesopelagic prey.
- $\delta^{13}C$ and $\delta^{15}N$ overestimated overlaps between trophic niches.
- Differences in foraging depth better explained resource partitioning.
- Foraging depth influenced mercury contamination level.

Table 1: Number of individuals, total length, C, N and Hg isotope composition, and total mercury concentration (THg) in muscles of blue, shortfin mako and smooth hammerhead sharks. Data are means (± standard deviation). THg is expressed on a dry weight basis. Different letters indicate significant differences between species for each variable.

Species	N	Total length (m)	$\delta^{13}C$ (‰)	$\delta^{15}N$ (‰)	$\Delta^{199}Hg$ (‰)	$\delta^{202}Hg$ (‰)	THg ($ng \cdot g^{-1}$)
Blue	13	1.98 (± 0.36)	-16.81 (± 0.91) ^{A}	18.15 (± 1.07) ^{A}	1.56 (± 0.10) ^{A}	0.63 (± 0.16) ^{AB}	7804 (± 2699) ^{A}
Shortfin mako	10	1.49 (± 0.43)	-16.36 (± 0.55) ^{A}	19.13 (± 1.10) ^{B}	1.94 (± 0.23) ^{B}	0.53 (± 0.15) ^{A}	4772 (± 3892) ^{B}
Smooth hammerhead	13	1.67 (± 0.16)	-16.25 (± 0.85) ^{A}	20.30 (± 0.60) ^{C}	1.82 (± 0.15) ^{B}	0.71 (± 0.12) ^{B}	3600 (± 1524) ^{B}

Table 2: Isotopic overlaps between blue, shortfin mako and smooth hammerhead sharks. Comparison is made between the SIBER ellipse metric for $\delta^{13}C$ and $\delta^{15}N$, SEA_B (Jackson et al., 2011), and the ellipsoid approach combining $\delta^{13}C$, $\delta^{15}N$ and $\Delta^{199}Hg$, SEV_B (Skinner et al., 2019).

	$\delta^{13}C/\delta^{15}N$	$\delta^{13}C/\delta^{15}N/\Delta^{199}Hg$
Blue | Shortfin mako	42.0%	23.0%
Shortfin mako | Smooth hammerhead	33.3%	27.4%
Blue | Smooth hammerhead	16.8%	12.9%

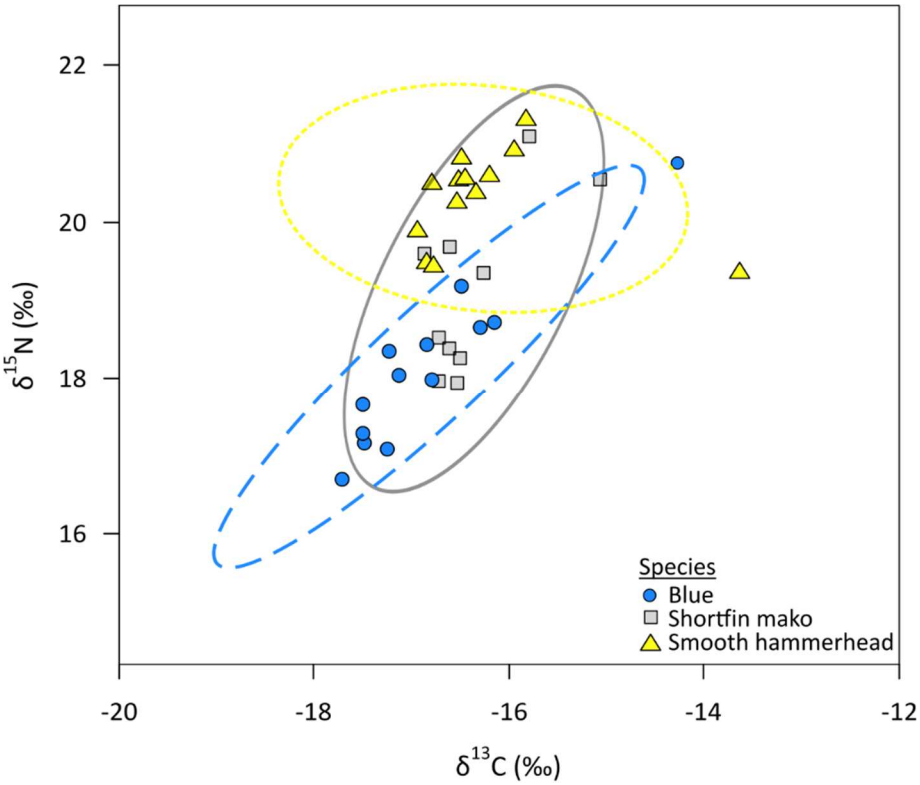

Figure 1: $\delta^{13}C$ and $\delta^{15}N$ of blue (● ----), shortfin mako (□ ——), and smooth hammerhead (△ ----------) sharks. The represented ellipses encompass 95% of the data.

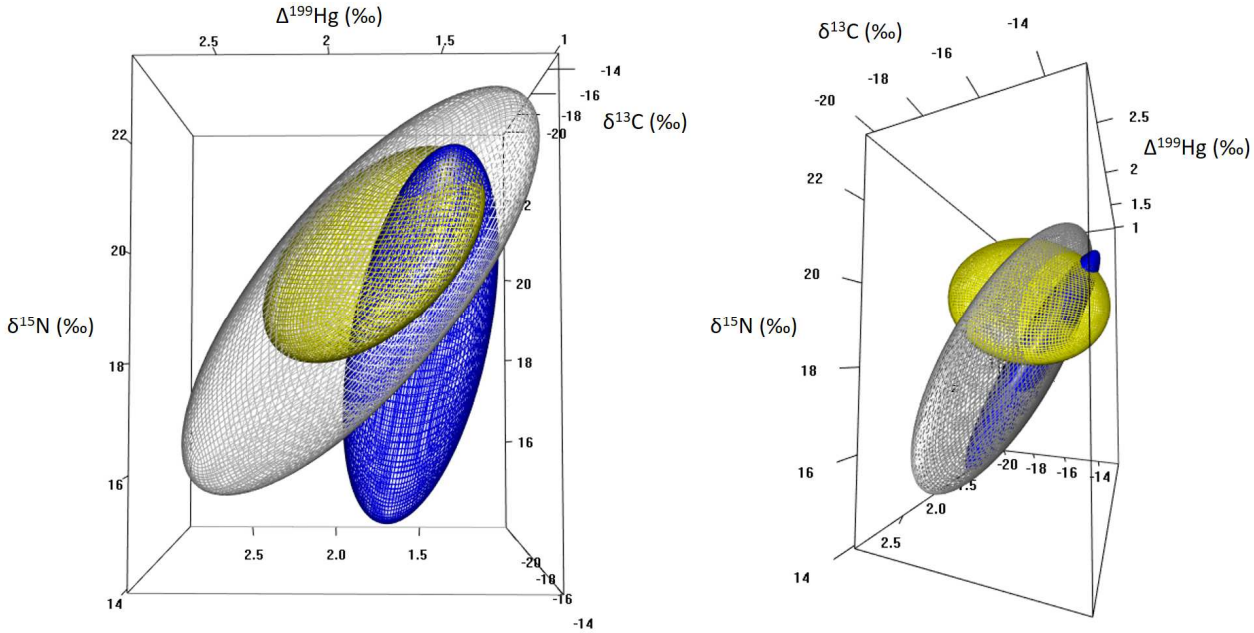

Figure 2: 95% ellipsoids using $\delta^{13}C$, $\delta^{15}N$ and $\Delta^{199}Hg$ for blue, shortfin mako and smooth hammerhead sharks respectively represented in blue, grey and yellow.

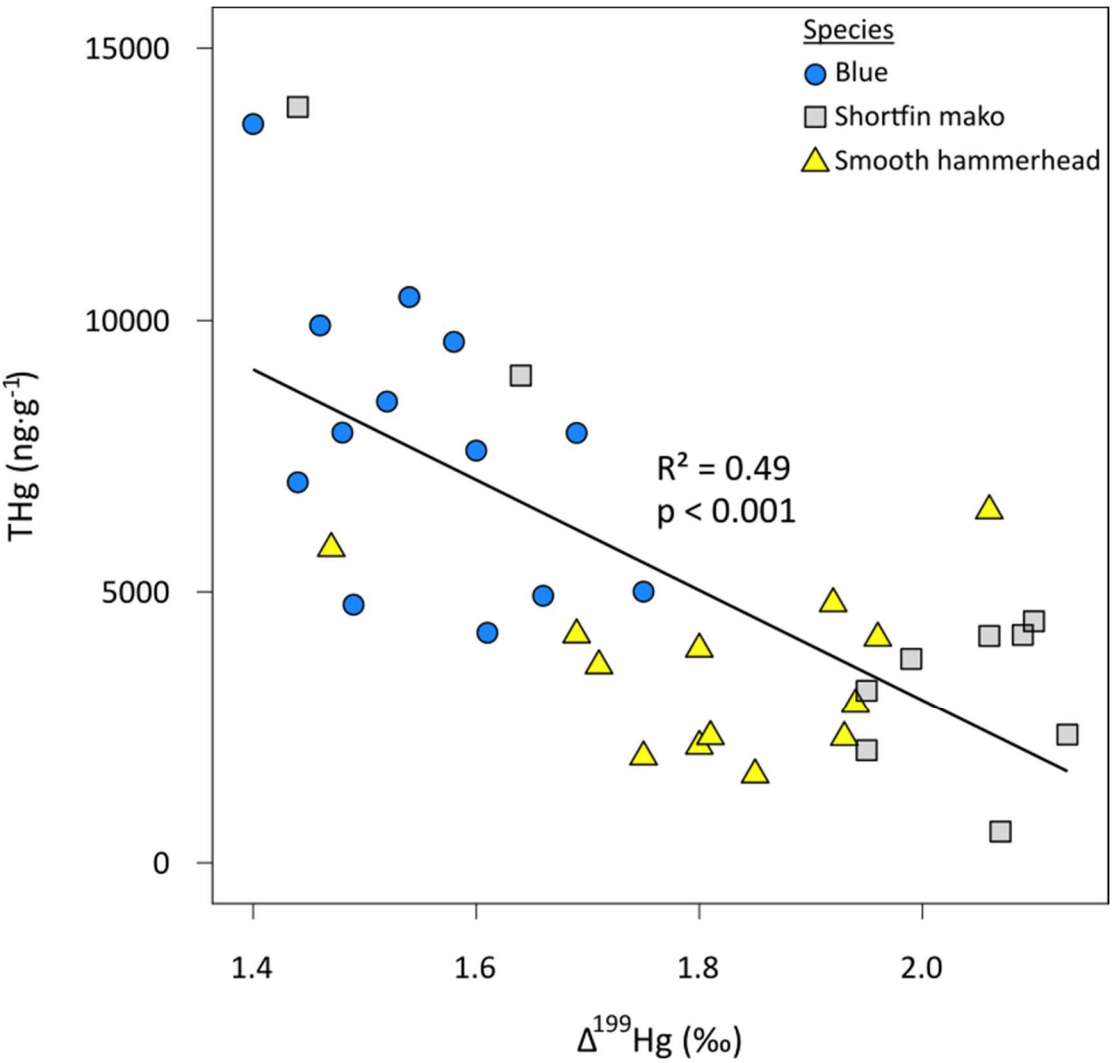

Figure 3: Variation of THg with Δ^{199}Hg values in the muscle of blue (●), shortfin mako (□) and smooth hammerhead (△) sharks. Data fit a linear curve. Pearson correlation (r^2 value) was significant as indicated by its p-value.